

PROCEEDINGS OF SPIE

[SPIDigitalLibrary.org/conference-proceedings-of-spie](https://spiedigitallibrary.org/conference-proceedings-of-spie)

NAOMI: the adaptive optics for the auxiliary telescopes of VLT

Frédéric Gonté, Sebastien Egner, Pierre Haguenaer, Julien Woillez, Emmanuel Aller-Carpentier, et al.

Frédéric Gonté, Sebastien Egner, Pierre Haguenaer, Julien Woillez, Emmanuel Aller-Carpentier, Jaime Alonso, Luigi Andolfato, Pierre Bourget, Pascaline Darré, Roderick Dembet, Christophe Dupuy, Pablo Gutierrez, Stefan Huber, Norbert Hubin, Jean-Paul Kirchbauer, Johann Kolb, Johan Kosmalski, Alexander Meister, Luca Pasquini, Javier Reyes, Pavel Shchekaturov, Nicolas Schuhler, Christian Stephan, Guillermo Valdes, Christophe Vérinaud, Jean-Philippe Berger, Jean-Baptiste Le Bouquin, Sylvain Guieu, Alain Delboulbé, Laurent Jocou, Yves Magnard, Thibaut Moulin, Sylvain Rochat, Eric Stadler, Peter Krempel, "NAOMI: the adaptive optics for the auxiliary telescopes of VLT," Proc. SPIE 10701, Optical and Infrared Interferometry and Imaging VI, 107010N (9 July 2018); doi: 10.1117/12.2312220

SPIE.

Event: SPIE Astronomical Telescopes + Instrumentation, 2018, Austin, Texas, United States

NAOMI: the adaptive optics for the auxiliary telescopes of VLTI

Frédéric Gonté^{*a}, Sebastian Egner^a, Pierre Haguenaer^a, Julien Woillez^a, Emmanuel Aller-Carpentier^a, Jaime Alonso^a, Luigi Andolfato^a, Pierre Bourget^a, Pascaline Darré^a, Roderick Dembet^a, Christophe Dupuy^a, Pablo Gutierrez^a, Stefan Huber^a, Norbert Hubin^a, Jean-Paul Kirchbauer^a, Johann Kolb^a, Johan Kosmalski^a, Alexander Meister^a, Luca Pasquini^a, Javier Reyes^a, Pavel Shchekaturov^a, Nicolas Schuhler^a, Christian Stephan^a, Guillermo Valdes^a, Christophe Vérinaud^a, Jean-Philippe Berger^b, Jean-Baptiste Le Bouquin^b, Sylvain Guieu^b, Alain Delboulbé^b, Laurent Jocu^b, Yves Magnard^b, Thibaut Moulin^b, Sylvain Rochat^b, Eric Stadler^b
Peter Kremp^c

^aEuropean Southern Observatory (Germany), ^bInstitut de Planétologie et d'Astrophysique de Grenoble (France), ^cKRP-Mechatec (Germany)

ABSTRACT

The New Adaptive Optics Module for Interferometry (NAOMI) is ready to be installed at the 1.8-metre Auxiliary Telescopes (ATs) at ESO Paranal. NAOMI will make the existing interferometer performance less dependent on the seeing conditions. Fed with higher and more stable Strehl, the fringe tracker will achieve the fringe stability necessary to reach the full performance of the second-generation instruments GRAVITY and MATISSE. All four ATs will be equipped between September and November 2018 with a Deformable mirror (ALPAO DM-241), a 4*4 Shack-Hartmann adaptive optics system operating in the visible and an RTC based on SPARTA Light. During the last 6 months thorough system test has been made in laboratory to demonstrate the Adaptive Optics and chopping capability of NAOMI.

Keywords: Adaptive Optics, Stellar Interferometry, Auxiliary Telescopes, Very Large Telescope Interferometer

1. INTRODUCTION

The New Adaptive Optics Module for Interferometry (NAOMI) will replace the fast tip-tilt correcting system implemented in the Coudé path of the ATs and equipped with a sensor called STRAP (System for Tip-tilt Removal with Avalanche Photodiodes) [1]. Its goal is to improve the delivered coherent flux when observing bright and intermediate magnitude object. It will improve the interferometric measurements of PIONIER[7], Gravity [5][6], and MATISSE[4] by increasing the number of coherent photos and then increase the overall efficiency. The project is led by the European Southern Observatory (ESO), in partnership with the Institut de Planétologie et d'Astrophysique de Grenoble (IPAG). NAOMI is the before last upgrade of the VLTI [8] for the 2nd generation of instrument the last one is Gra4MAT [8] and will be implemented in 2019.

The four Auxiliary Telescopes [2] will be equipped with a NAOMI system between September and November 2018. The Figure 1 (left) shows one of the four Auxiliary Telescopes on the station C0 of the Very Large Telescope Interferometer. It is mainly composed of 3 parts. From top to bottom, first the telescope, then the transporter and last the Relay Optics Structure laying beneath the telescope to provide the optical beam to the Interferometer. The Telescope is composed of 3 mirrors and the Coude path is composed of 5 mirrors. The pupil of the telescope is re-imaged on M6 which is the fast steering mirror which will be replaced by the Corrective Optics of NAOMI.

*fgonte@eso.org; phone 0049 89 3200 6191 eso.org

2. NAOMI INTERFACES WITH THE AUXILIARY TELESCOPES AND THE VERY LARGE TELESCOPE INTERFEROMETER

NAOMI is integrated to an existing system and as such makes it very complex. Few example are shown here. Figure 1 (center and right) shows the different areas in which NAOMI will be physically implemented. The Corrective Optics replaces the M6 mirror position at the level of the azimuth of the telescope. The wavefront sensor and its relay optics are implemented in the lower part of the Relay Optical Structure (ROS) and replaces the STRAP sensor. The electronics are also implemented in several areas, one cabinet goes at the azimuth level, another other goes in the ROS. The last one and the RTC electronics goes in the Signal Cabinet implemented in the Transporter. NAOMI is also connected to remote workstation and data server implemented respectively in 2 different Computer Room. The first one being in the VLT Control Building and the second one in the VLTI building as seen on Figure 2. The NAOMI software is interfaced the same way as the STRAP system with the Auxiliary Telescope and the VLTI Instrument Supervisor System.

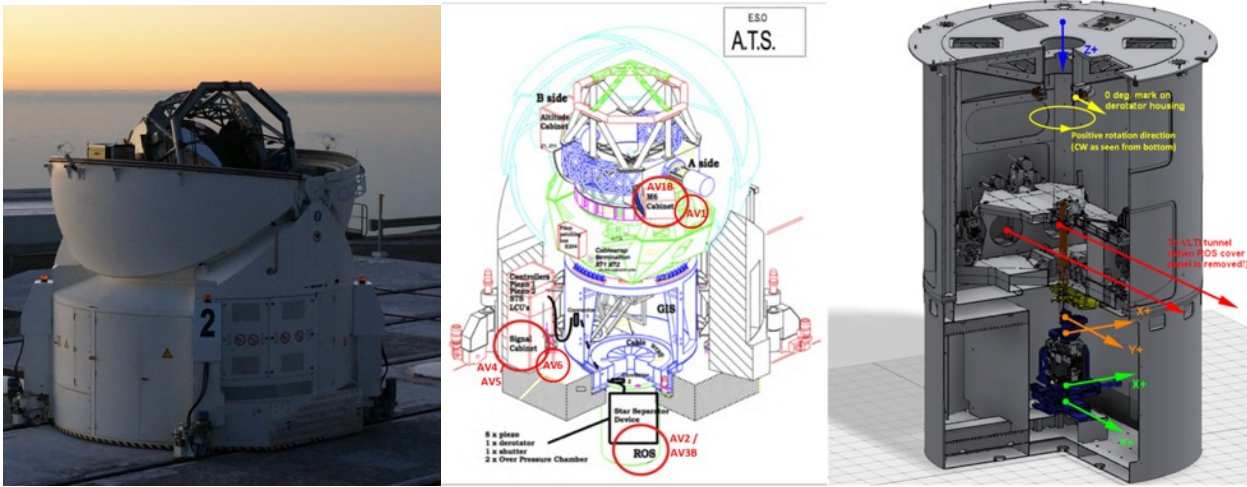


Figure 1: (left) AT2 on the C0 station of the Very Large Telescope Interferometer (center) cut view of the AT and (right) cut view of the ROS with including in it the STar Separator. The NAOMI WFS lays under the STS.

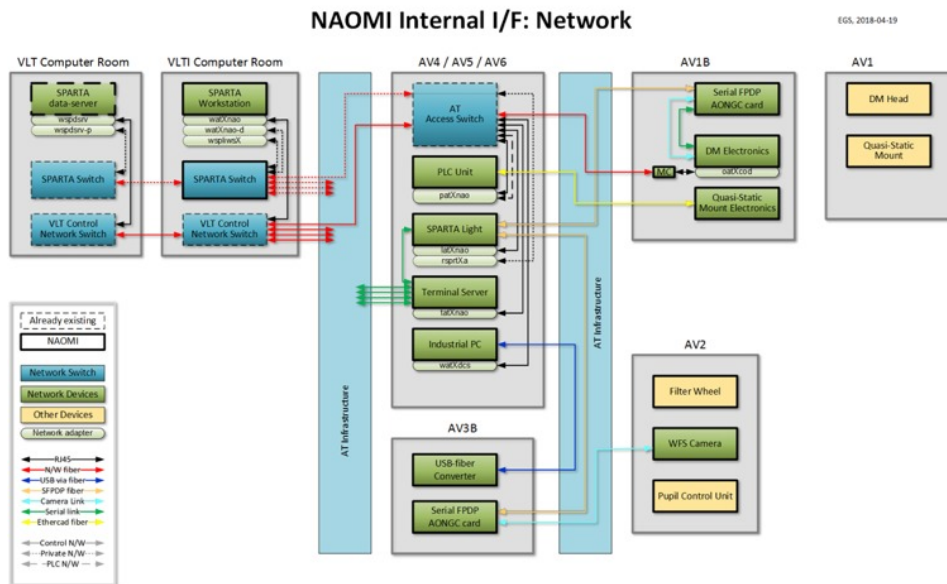


Figure 2: NAOMI network interfaces showing the connection to the VLT and VLTI Computer room.

3. NAOMI SOFTWARE AND AUXILIARY TELESCOPE CONTROL SOFTWARE

NAOMI software is a component of the Auxiliary Telescope control software. It is composed of 4 parts, the Telescope Control Software, the Instrument Control software, the RTC and finally the Detector Control Software. It is implemented in three hierarchical layers as seen on Figure 3.

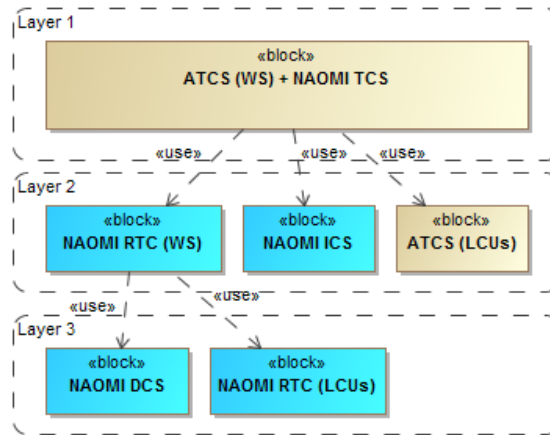


Figure 3: Control Hierarchy Layers: distribution of ATCS and NAOMI SW components

The NAOMI software is deployed on three workstations and one Local Control Unit as shown on the Figure 4

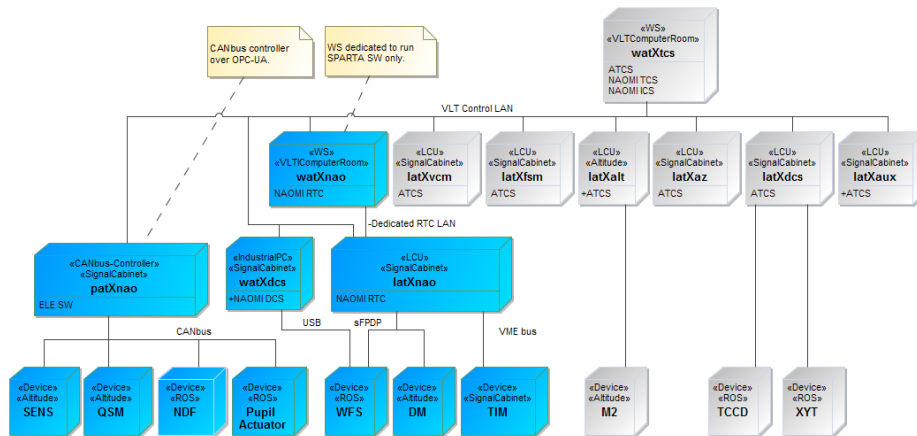


Figure 4: NAOMI computational nodes («WS», «LCU» stereotypes) and controlled devices («Device» stereotype) are shown in blue. NAOMI SW components deployed on each computational node are shown as attributes: NAOMI TCS, NAOMI ICS, NAOMI RTC, and NAOMI DCS. Physical location of the computational nodes and devices are labelled with «VLTComputerRoom», «VLTICComputerRoom», «SignalCabinet», «ROS», «Altitude» stereotypes.

4. REAL TIME CONTROL

The NAOMI RTC is based on the light version of SPARTA [3] on two elements. The First one is a ESO standard Linux Instrument Workstation (watXnao). The Second element is the real time processing pipeline called the RTC box. This box is composed of an 19" VME 64 crate having; one real time single board computer (rsprtXa) composed of a MVME6100 VME64 board and two Curtiss-Wright fibreXtreme SL240 PMC/XMC cards). An ESO TIM board and a standard Local Control Unit (latXnao) composed of one MVME6100 VME64 board.

The last component common to all NAOMI SPARTA systems is the SPARTA Data server. The Figure 5 shows the HW block diagram for NAOMI.

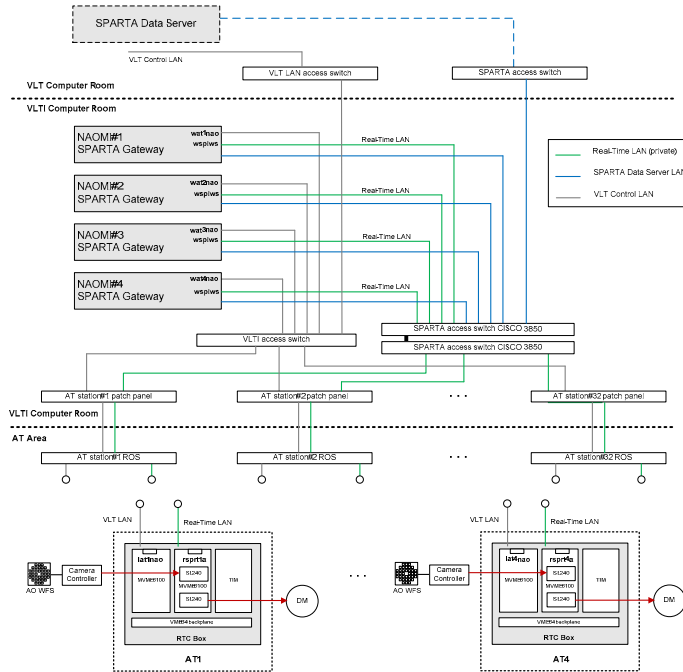


Figure 5: NAOMI RTC Hardware Block Diagram

The RTC Box design is based on 3 pipelines processing stages; the Wavefront Processing, the Wavefront reconstruction and the Control.

The Wavefront processing unit manages a window at 64×64 meta-pixels on a 4×4 sub-aperture geometry and depending of the mode will use 2 different sub-aperture window size of 6×6 pixels (in closed loop) of 16×16 (in acquisition mode). The block diagram for the WPU is given in Figure 6.

The wavefront reconstruction is performed by Matrix Vector Multiplication delivering a result in the modal space. It is based on 12 sub-aperture for the WFS. The system can reconstruct up to 21 modes but NAOMI system delivers its best performances with 14 modes.

The control is based on 2 driver; the Infinite Impulse Response driver and the Anti Vibration Control driver. The IIR driver takes care of the AO loop and of the chopping when the AVC driver focus on rejecting vibrations at particular frequencies. The IIR block diagram is shown on Figure 7.

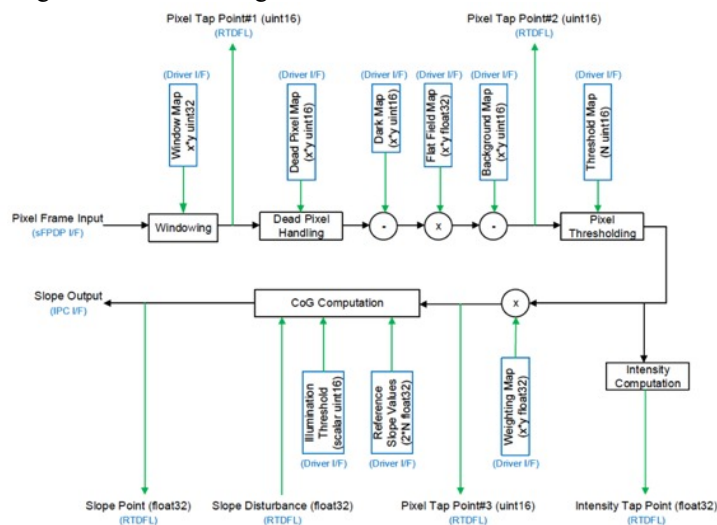


Figure 6: NAOMI RTC WPU Block Diagram: x, y stand for the dimensions of the WFS ROI (64×64 pixels); N stands for the number of WFS used sub-apertures (12)

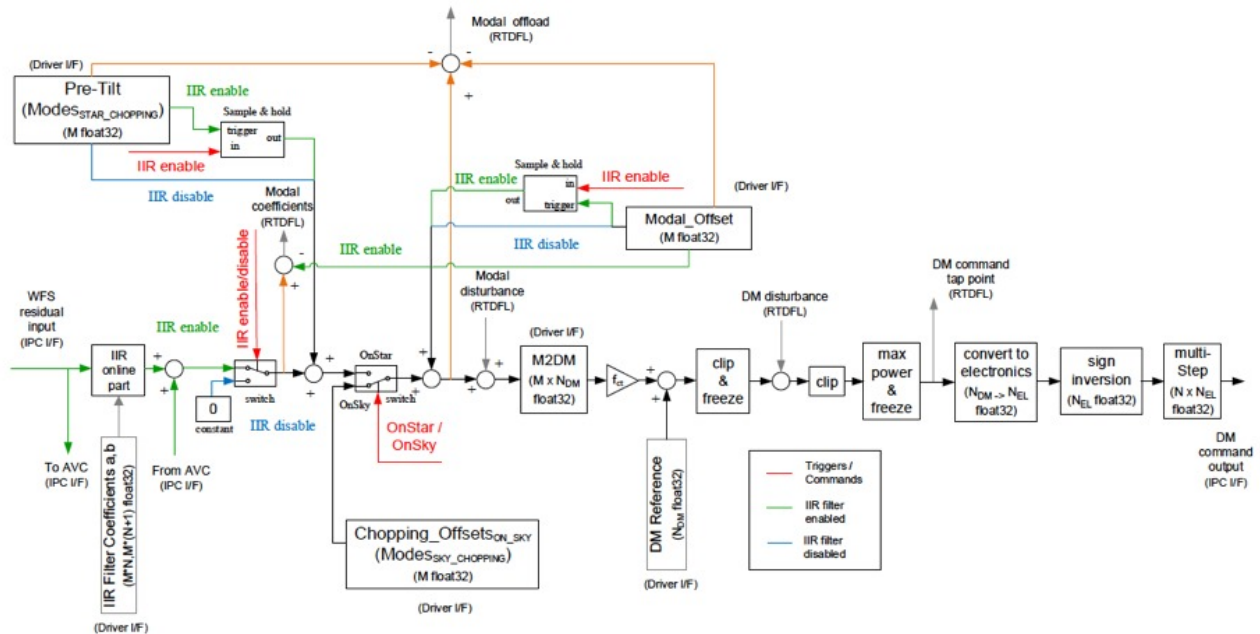


Figure 7: NAOMI RTC Box IIR Block Diagram: M stands for the number of controlled modes (14); N_{DM} stands for the number of used DM actuators (241); N_{EL} total number of actuators expected by DM electronics; N number of steps

A pre-tilt is made on the mirror before the start of the chopping. It can run a chopping at up to 5Hz. The block diagram for the open loop chopping is shown on Figure 8.

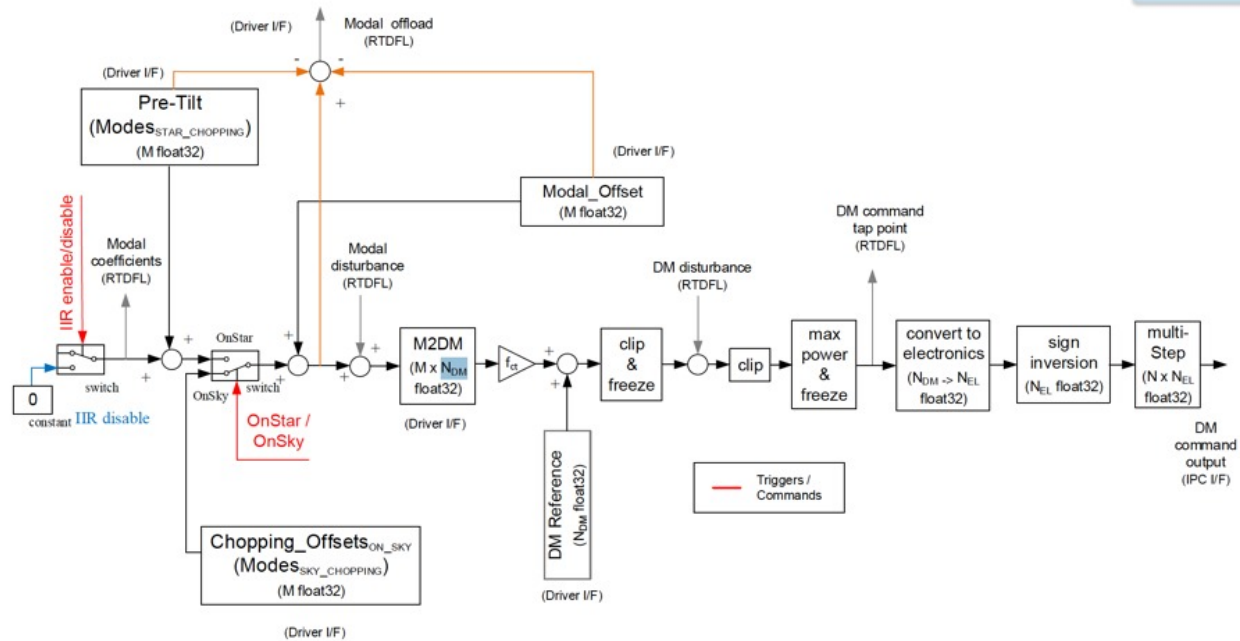


Figure 8: NAOMI RTC Box IIR open loop Chopping Block Diagram

5. CORRECTIVE OPTICS

NAOMI corrective optics is developed by IPAG in collaboration with ESO. It consists of a deformable mirror (ALPAO DM-241) mounted on a quasi-static Gimbal mount. The deformable mirror compensates for all wavefront errors and provides the chopping. The Gimbal mount provides motorized tip-tilt adjustment needed for the alignment (see Figure 9).

The Deformable Mirror ALPAO DM241 has a silicium membrane and magnets/coil acting as actuators. The magnet are fixed on polymer springs. The main qualities of these mirrors are high linearity, low hysteresis and large stroke. Their main weakness are creep, overshoot. The stroke is also linear to temperature in the range used for NAOMI on Paranal (1 to 20 degC).

The ALPAO DM241 provides the chopping and atmospheric turbulence correction capability. The device has a tip-tilt wavefront stroke of up to 50 μm PtV at ambient temperature. Its capability decreases linearly at lower temperature. This is calibrated in NAOMI. Piston stability and control is the second feature to study when a DM is used for interferometric purposes. The piston introduced by the DM is estimated by the influence functions calibrated in the laboratory. the DM shape is controlled piston-free to few percent. Even though the influence functions are expected to evolve with time, the piston ratio, (influence function piston over piston-free influence function amplitudes) is assumed to remain constant, hence the need of external measurement devices in operation is not foreseen.

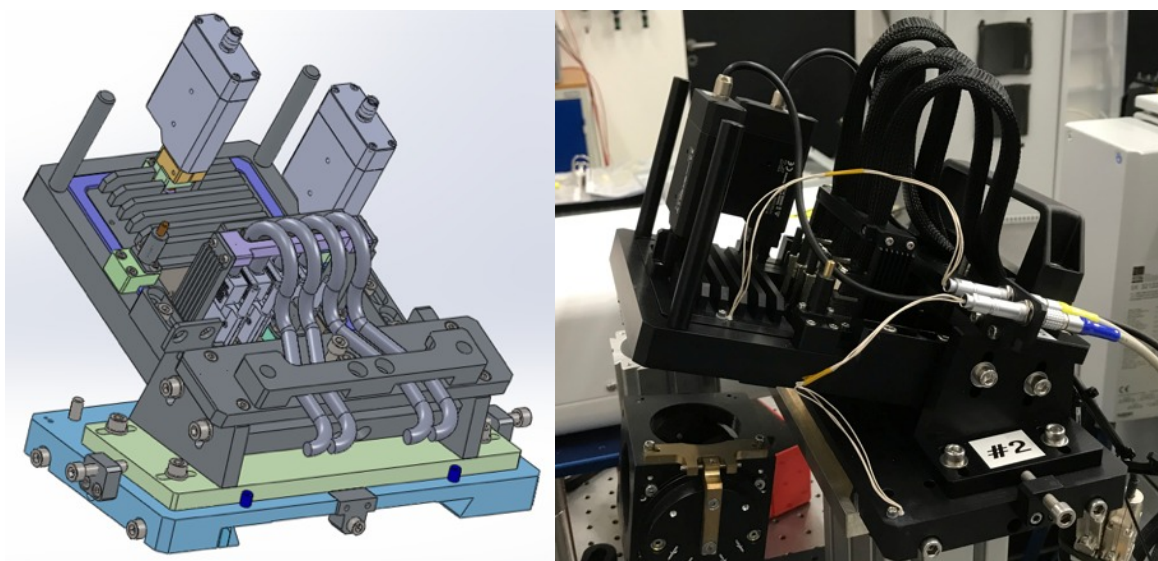


Figure 9: (left) 3D model of the Corrective Optics, (right) photo of the C.O. on a test bench.

The deformable mirror needs to provide sufficient stroke to compensate for; atmospheric disturbance (Atmospheric tip-tilt and higher modes. It includes also the effect of the dome seeing at low ground wind speeds), windshake effect on the telescope, Telescope quasi-static errors (Telescope wavefront errors (especially defocus) that evolves during the night due to altitude and thermal variations in the tube. The deformable mirror does not need to compensate for tip-tilt quasi-static errors as those will be off-loaded to the telescope axis.), chopping (The deformable mirror will be used for chopping for the MATISSE [4] instrument) and VLTI offset (defocus offset sent by the VLTI instruments).

A computation of the stroke budget is given in Table 1The required maximum stroke is 23.33 μm PTV on the pupil.

Mode	Component	Requirement	DM Stroke (PtV in μm)
Tip-Tilt	Chopping	+/- 2.25"	9.82
	Atmospheric tip-tilt	Seeing 1.4"	3.94
	Telescope tracking error	0.1"	1.09
	Telescope Wind Check	0.4"	0.87
	VLTI Tip/Tilt Offsets	n/a	0

High-Order	Chopping Accuracy	n/a	0
	Sub-total+10% margin		17.3
	Atmospheric High-Order	Seeing 1.4''	3.21
	Telescope focus	WFE=13 nm RMS/min	0.68
	Telescope Static Aberrations	WFE=300 nm RMS	0.75
	VLTI Focus offset	WFE=200 nm RMS	0.85
	Subtotal+10% margin		6.03
	Total		23.33

Table 1: Stroke requirements for the Corrective Optics split in different contributors.

Figure 10 shows the 21s modes measured on one of the 5 deformable mirrors delivered for NAOMI as well as the best obtained flat with a Wavefront of 14 nm RMS.

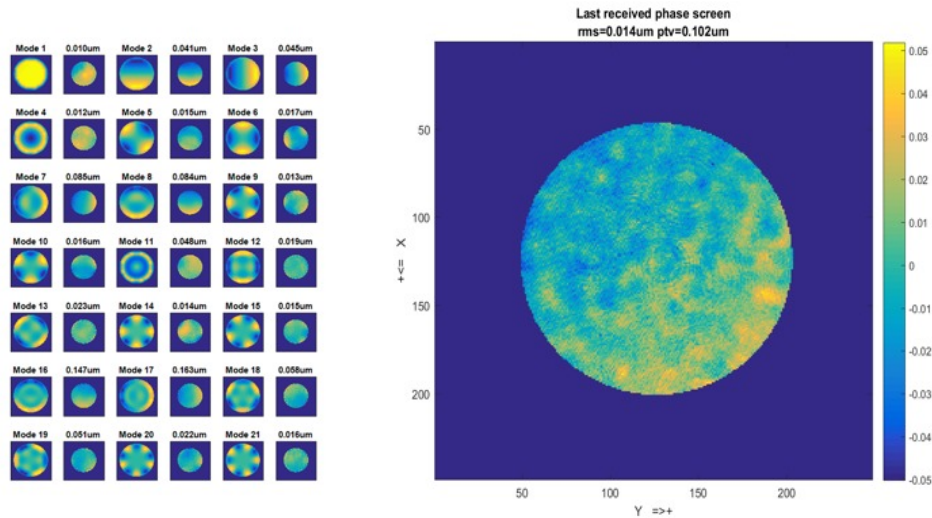


Figure 10: (left) the 21st modes measured on one of the 5 deformable mirrors produced for NAOMI. (right) best flat obtained using a high density SHS.

6. WAVEFRONT SENSOR

The Wavefront sensor is a 4*4 SHS with 12 sub-aperture being used. It works in the visible (450 to 900 nm). A pupil tracker unit is integrated on it to correct the pupil position which can move by up to 15% of the size of the pupil. The pupil de-rotation is made by software. The WFS is also integrated on Field stabilization stages to pick up the correct field and compensate the move of the field seen by the WFS when compensating the pupil position.

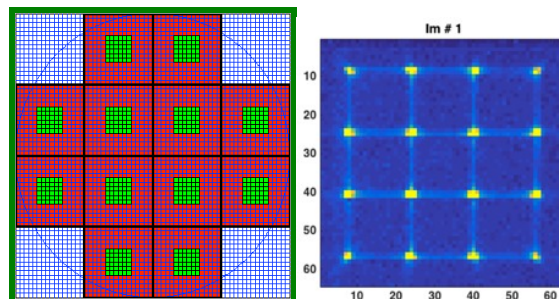


Figure 11: (Left): SHS configuration maps with in red the 16x16 pixels used in the full-geometry configuration, in green the 6x6 pixels used in the AO-geometry. (right): WFS acquisition with Flat reference

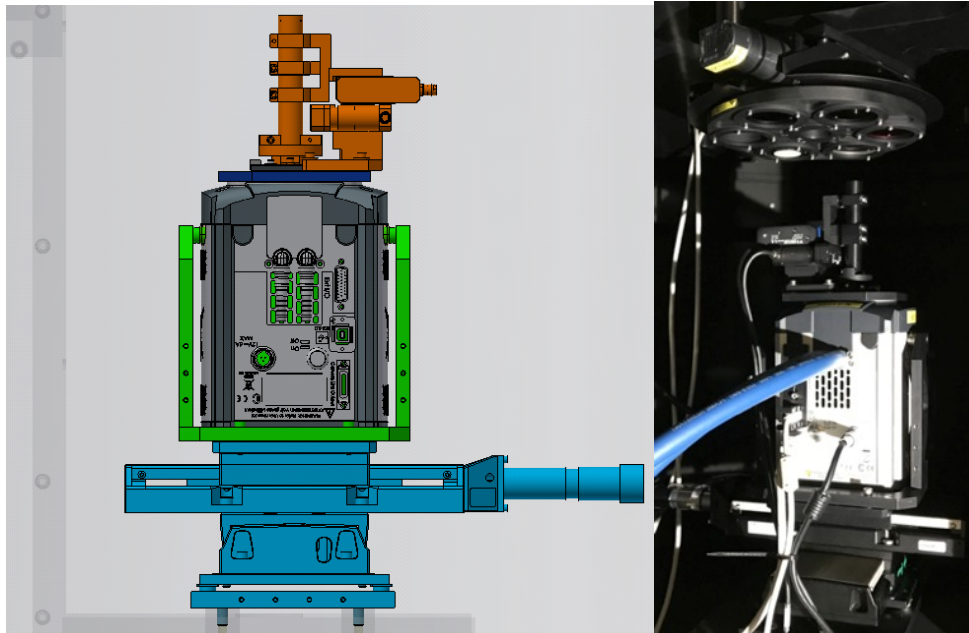


Figure 12: (left) WFS assembly. starting from the top: the PCU in brown, the lenslet mount in deep blue, the camera in grey, the Detector Assembly interfacing in green with the Field Stabilization stages in blue, (right) photo of the WFS in the test bench and with the Neutral Density Filter Wheel on top of it.

The detector selected for NAOMI is a commercial electro-multiplicative CCD camera: ANDOR ixon ultra 897. The camera has a chip with 512x512 pixels with a pixel size of 16 μm . To increase the frame speed and the pixel size the camera will be operated in a 2x2 binned mode (implemented at low level). This means a camera of 256x256 mega-pixels and pixel size of 32x32 μm . This implies a pupil size diameter of 2.048 mm for the pupil area of 64x64 mega-pixels. The area of interest will be read in a customized crop window mode in order to read the detector at the required speed (500 Hz). The camera offers a RON $< 1 e^-$ when the EM gain (L3 gain) is applied. Gain factors up to 1000 can be applied. The dark of the camera has been measured with different gain and frequencies as seen on Figure 13 for one of the modes used by NAOMI. The figure shows the mean of all frames, the standard deviation of the frames from which the mean has been subtracted, and the histogram of the darks frames values are given.

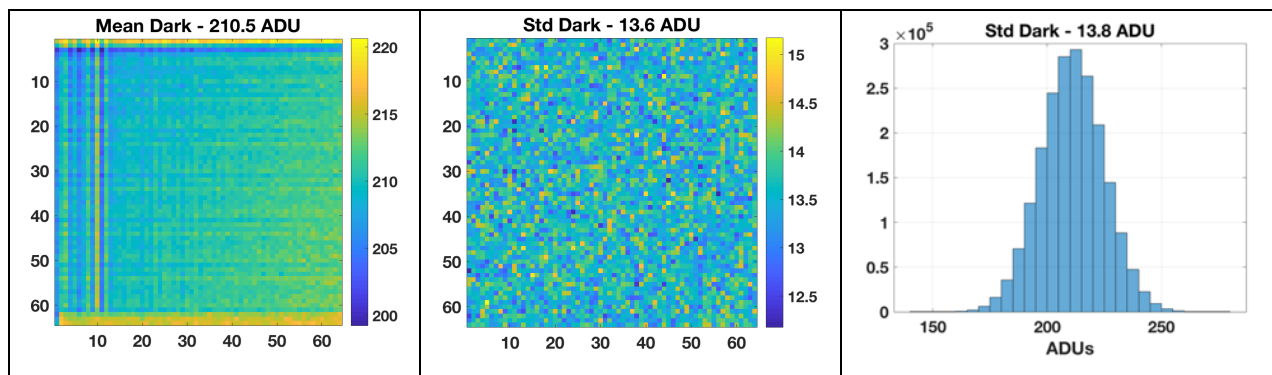


Figure 13: WFS mode#2 with acquisition frequency at 500Hz and EM gain=3

7. SYSTEM TEST RESULTS

The system test has been made on a test bench simulating the Auxiliary Telescope including the ROS. The turbulences have been produced by the Deformable mirror itself using a bases of 120 modes. Basically 10 times more than what is used for the correction (14 modes)

The transfer functions of the system has been measured and compared to the theoretical one as seen in Figure 14. The linearity of the system has also been measured as seen in Figure 15.

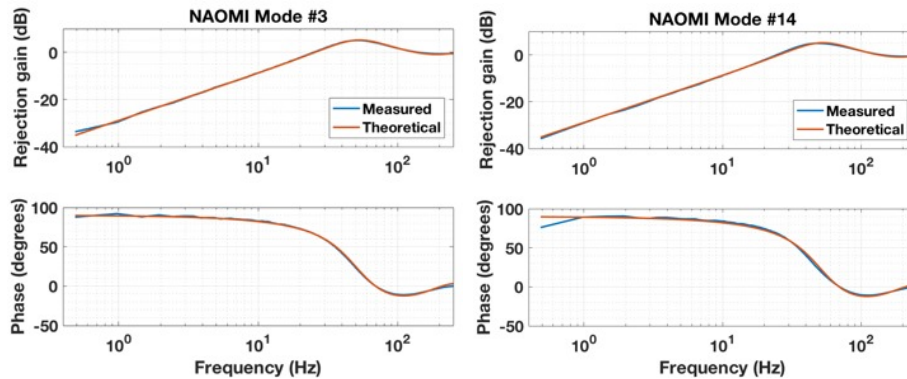


Figure 14: Transfer function for DM mode 3 (focus) and mode 14.

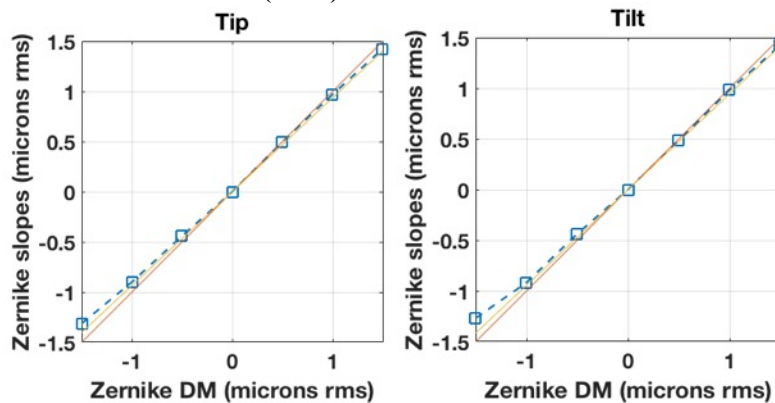


Figure 15: : Tip (Left) and Tilt (right) slope between the Zernike values computed from the WFS slopes vs the Zernike values computed from the DM commands

The ratio of correction on turbulences has been measured. The rejection functions are very similar for the 14 modes, and in these simulated atmosphere conditions that are close to the limit ones specified for NAOMI, the cut-off frequency is around 23 Hz. The Figure 16 shows the ration of the PSD between closed loop and open loop for the 14 modes used by NAOMI. Figure 17 shows the same ratio for 5 different rotation of pupil. It demonstrate the efficiency of the numerical de-rotation implemented in NAOMI.

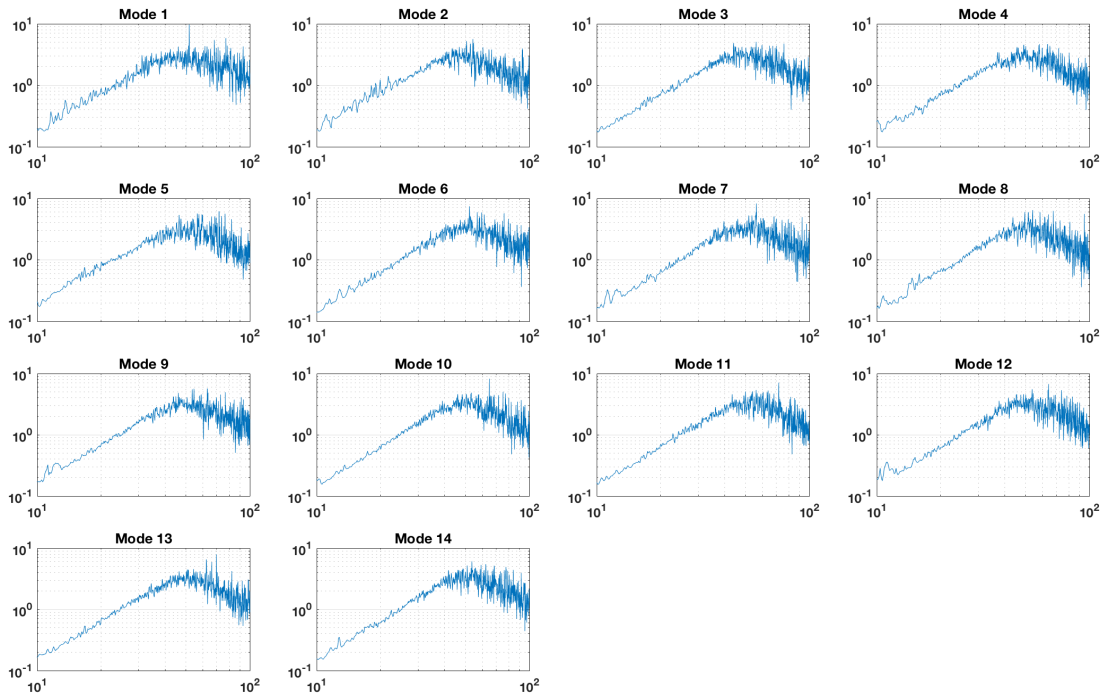


Figure 16: Ratio of the PSD in CL and OL for turbulence injected on the DM (equivalent to 1.4'' seeing).

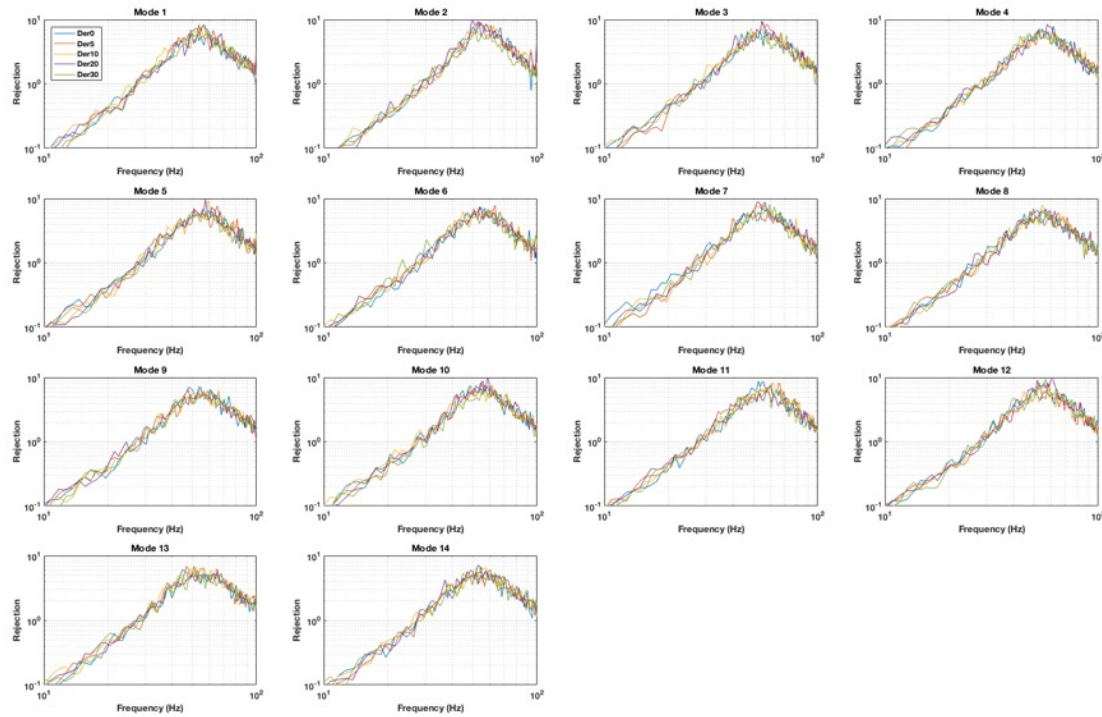


Figure 17: OL/CL rejection functions of the 14 corrected modes and for 5 position of the derotator implemented in the test bench to produce the rotation of pupil which will be seen by the WFS of NAOMI once implemented in the AT.

Figure 18 shows the Strehl ratio performance in the H band for different modes and different flux for a seeing of 1.1". It shows that the performance is better than 55% of Strehl ratio in high flux. NAOMI also obtain a tip-tilt residual better than 150 milliarcsec in faint mode (1 photon/sub-aperture/ms).

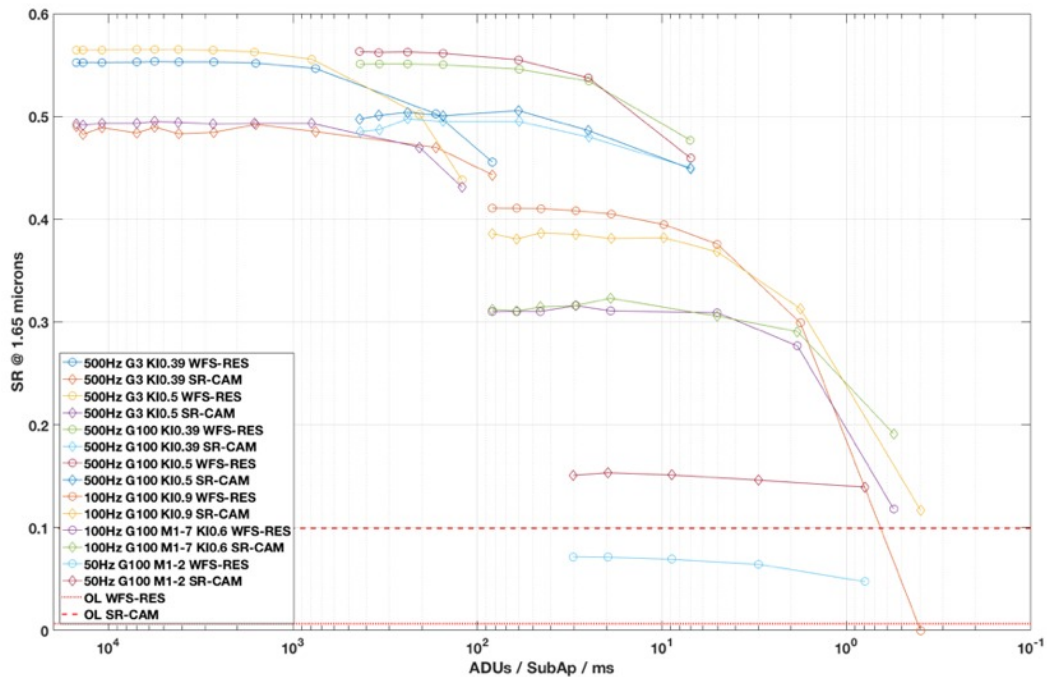


Figure 18: SR vs flux for the different NAOMI modes and AO loop configurations. Seeing = 1.1", Tau0 = 2.5 ms.

The most important parameter for NAOMI is probably its capacity to inject constant flux in the spatial filters or the fibers of the interferometric instruments. The performances are shown on Figure 19 and compared to an open loop system and to a pure tip-tilt corrector system (equivalent to STRAP). It is clearly seen that we have a much higher coupling efficiency and much more stable.

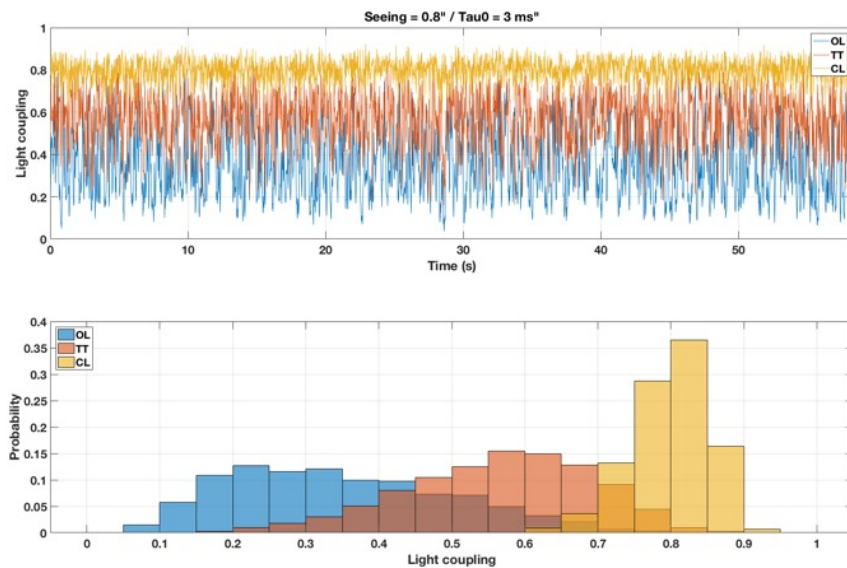


Figure 19: Injection Flux obtained with 0.8" seeing when NAOMI is in Open Loop, in closed loop only with the Tip-tilt mode (equivalent to STRAP) and in standard closed loop

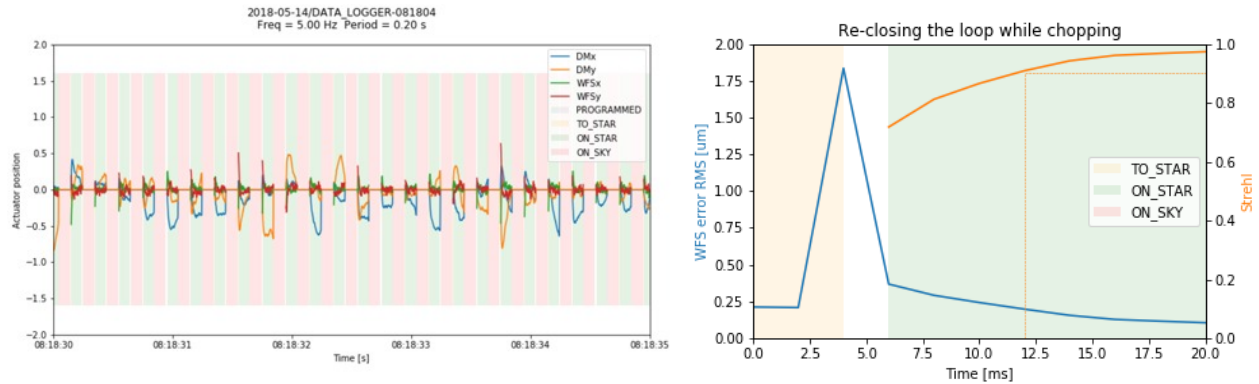


Figure 20: (left) Closed-loop chopping performance with turbulence. Only the TipTilt content of DM and the WFS are shown. Chopping was configured with a frequency of 5 Hz and a stroke of 6 arcsec. The DM is in a fixed position when ON_SKY and correct the turbulence when ON_STAR.. (right) performance of NAOMI reclosing the loop

8. CONCLUSION

The four Auxiliary Telescopes will be upgraded with NAOMI between September and November 2018. This is the before last system to be implemented in the context of the upgrade of the VLTI for the 2nd Generation of Instruments. NAOMI will improve substantially the precision of the interferometric measurements and the performance of the fringe tracking by making the coherent flux stay, at all time, above a minimum threshold. It will also provide a chopping capability of 5 Hz with an amplitude of up to 6" and re-closing the loop in less than 20ms. It provides the increase of performance to exploit at best the 2nd generation of instruments during the next decade[9].

REFERENCES

- [1] Bonaccini, D.; et al.; "STRAP for the VLT Instruments," Proc. SPIE 3126, (1997)
- [2] Koehler, B.; Flebus C.; "VLTI auxiliary telescopes," Proc. SPIE 4006, (2000)
- [3] Suarez, M.; et al.: "SPARTA for the VLT: status and plans," Proc. SPIE. 8447, (2012)
- [4] Lopez, B.; et al.: "The MATISSE instrument at the VLTI", SPIE 10701, 2018
- [5] Eisenhauer, F.; et al "GRAVITY:" a new era for optical interferometry" SPIE 10701 (2018)
- [6] Eisenhauer, F; et al "Breaking the limits: early science with the GRAVITY interferometer", SPIE 10702, 2018
- [7] Bourget, P.; et al.: "How to create space in the VLTI: PIONIER 3D project," Proc. SPIE 9907, (2016)
- [8] Woillez, J, et al.: " VLTI status update: two years into the 2nd generation" SPIE 10701, 2018
- [9] Merand, A.; et al.: "The VLTI roadmap for the next decade" SPIE 10701, 2018